Simple and Fast Polarization Tracking algorithm for Continuous-Variable Quantum Key Distribution System

Yan Pan, Heng Wang, Yun Shao, Yaodi Pi, Ting Ye, Yang Li, Wei Huang*, and Bingjie Xu**
Science and Technology on Communication Security Laboratory, Institute of Southwestern Communication, Chengdu 610041, China
**huangwei096505@aliyun.com, **xbjpku@163.com*

Abstract: A simple and fast polarization tracking algorithm for pilot tone-assisted CV-QKD system is demonstrated. Experimental results show that the proposed algorithm can track polarization scrambling rate ≥12.57 krad/s with a good performance. © 2022 Authors
OCIS codes: (270.0270) Quantum optics; (270.5568) Quantum cryptography; (270.5585) Quantum information and processing

1. Introduction

With the rapid development of advanced computing strategies, the traditional encryption technology that mainly depends on computational complexity becomes hard to guarantee the security of high-security required fiber-optical communication systems. The continuous-variable quantum key distribution (CV-QKD) with information theoreticaly security, which is compatibility with optical communication networks, becomes a prime candidate to deal with the security threats [1]. In this case, a lot of protocols and schemes have been proposed, among which the local local oscillator (LLO) CV-QKD with Gaussian modulated or distrete modulated coherent state protocol is a promising scheme for practical application. For LLO CV-QKD, an independent free-running laser is used as the local oscillator, which has uncorrelated phase, wavelength and polarization compared to the laser at the transmitter. Because of the random birefringence of the standard single-mode fiber (SSMF), the variation of the state of polarization (SOP) is drastic and random [2], and the rapid fluctuations of the SOP will significantly deteriorate the performance of the CV-QKD system. Thus, the SOP of LLO CV-QKD system needs to be manipulated, and many optical or digital methods are proposed [3-5]. Among them, due to flexibility, effectiveness, and low insert loss, digital methods such as the constant modulus algorithm (CMA), Kalman filter and Stokes space-based polarization tracking algorithm are studied for CV-QKD. However, the complexity of above-mentioned algorithms is high, where the demonstrated polarization tracking rate for CV-QKD is limited to krad/s.

In this work, a simple and fast polarization tracking algorithm is proposed for LLO CV-QKD system. Instead of multiple iterations, the proposed algorithm calculates the inverse Jones matrix by pilot tone directly. Therefore, compared to CMA, Kalman filter and Stokes space-based polarization demultiplexing algorithms, the complexity of the proposed algorithm is low. Experimental results of 1 GBaud discrete modulated LLO CV-QKD system with 25 km SSMF link are given, and the results of excess noise and secret key rates (SKRs) show that the proposed algorithm recover quantum signal effectively. Furthermore, to evaluate the polarization tracking performance, experiments at various scrambling rates are performed. The experimental results show that the proposed algorithm can track SOP scrambling of ≥12.57 krad/s with limited decrease of SKR.

2. Principle

The principle of the proposed algorithm is shown in Fig.1. At the transmitter, the quantum signal with discrete modulated coherent-state (DMCS) and pilot tone 1 (PT1) are modulated at vertical polarization, and the center frequency of PT1 is f_1. Here, the discrete Gaussian (DG) 256QAM quantum signal is used under the security framework of Ref. [6]. The pilot tone 2 (PT2) is modulated at horizontal polarization, and the center frequency of PT2 is f_2. Denoting the Jones vector of the multiplexed signal as $\left[E_Q^{Tx}(t)+E_{P1}^{Tx}(t); E_{P2}^{Tx}(t)\right]^T$. Then, the multiplexed signal is launched into the optical fiber link. Assuming the polarization characteristics of the optical fiber link can be represented by a unitary Jones matrix J as described in Ref. [7], the received optical signal can be expressed by

$$\begin{bmatrix} E_X^{Rx}(t) \\ E_Y^{Rx}(t) \end{bmatrix} = J \times \begin{bmatrix} E_Q^{Tx}(t)+E_{P1}^{Tx}(t) \\ E_{P2}^{Tx}(t) \end{bmatrix}, \qquad where \quad J = \begin{bmatrix} \cos\alpha(t)\exp(j\varphi_1(t)) & -\sin\alpha(t)\exp(j\varphi_2(t)) \\ \sin\alpha(t)\exp(-j\varphi_2(t)) & \cos\alpha(t)\exp(-j\varphi_1(t)) \end{bmatrix} \tag{1}$$

$\alpha(t)$ is the polarization rotation angle, $\varphi_1(t)$ and $\varphi_2(t)$ are the rotation phase angles. Hence, $\alpha(t)$, $\varphi_1(t)$ and $\varphi_2(t)$ are the key for polarization tracking. Here, the following model is performed to demultiplexing the quantum and pilot signal

$$\begin{bmatrix} \cos\alpha(t)\exp(j\Delta\varphi(t)/2) & \sin\alpha(t)\exp(-j\Delta\varphi(t)/2) \\ -\sin\alpha(t)\exp(j\Delta\varphi(t)/2) & \cos\alpha(t)\exp(-j\Delta\varphi(t)/2) \end{bmatrix} \times \begin{bmatrix} E_X^{Rx}(t) \\ E_Y^{Rx}(t) \end{bmatrix} = \begin{bmatrix} \exp(j\phi(t)) & 0 \\ 0 & \exp(-j\phi(t)) \end{bmatrix} \begin{bmatrix} E_Q^{Tx}(t)+E_{P1}^{Tx}(t) \\ E_{P2}^{Tx}(t) \end{bmatrix} \tag{2}$$

where $\Delta\varphi(t)$=-[$\varphi_1(t)$+$\varphi_2(t)$]/2, and $\phi(t)$=[$\varphi_1(t)$-$\varphi_2(t)$]/2. As can be seen from Eq. (2), the quantum signal $E_Q^{Tx}(t)$ is demultiplexed to the vertical polarization, and the residual phase noise $\phi(t)$ can be compensated by PT1. The offline DSP mainly includes 1) Bandpass filtering. A frequency-domain ideal bandpass filter is used to split quantum signal, PT1 and PT2. 2) Digital *x*/*p* demodulation. The frequency estimation, down-conversion and lowpass filtering are performed to obtain *x* and *p* quadrature from the intermediate frequency signal digitally. 3) Fast polarization tracking. As can be seen from Eq. (2), the key of polarization tracking is $\alpha(t)$ and $\Delta\varphi(t)$. Using PT2 in Eq. (1), $\Delta\varphi(t)$ can be achieved by calculating the angle of $E_P^Y(t)\bullet\left(E_P^X(t)\right)^*$, and $\alpha(t)$ can be achieved by $\arctan\left(-E_P^X(t)/E_P^Y(t)\bullet\exp(j\Delta\varphi(t))\right)$. $E_P^Y(t)$ and $E_P^X(t)$ are achieved PT2 after bandpass filtering. 4) Phase noise compensation. The phase noises are estimated from the demultiplexed PT1 and PT2 for vertical and horizontal polarization, respectively, and the phase noises of the quantum signals can be compensated. 5) data-aided equalization. With the help of the training sequence and least-mean-square (LMS) algorithm, a real-valued FIR filter is implemented to compensate the residual noise and slow polarization variation. After the above processing, the raw kay signal $\hat{E}_Q^{Tx}(t)$ is obtained.

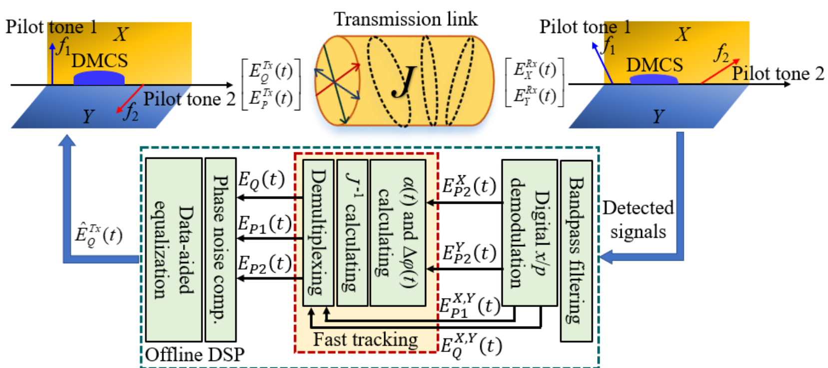

Fig. 1. The principle of the propsoed polarization tracking algorithm. comp., compensation.

3. Experimental setup, results and discussion

Figure 2 shows the experimental setup of the LLO CV-QKD to evaluate the performance of the proposed algorithm. At Alice's site, a continuous-wave laser (i.e., CW laser 1) with a linewidth of <100 Hz is used as the carrier, and the wavelength is set to 1550.22 nm. Then, the light is split into two branches by a polarization beam splitter (PBS). One branch of the optical carrier is modulated by an In-phase/quadrature modulator (IQ modulator). The *x* and *p* quadrature signals with an 850 MHz frequency shift are generated by a two channels arbitrary waveform generator (AWG) that works at 30 GSa/s, and the two electrical signals are amplified by two amplifiers for driving the IQ modulator. Here, PT1 with 850 MHz frequency shift from the center frequency of the quantum signal is modulated, and the symbol rate of the quantum signal (i.e., DG-256QAM) is set to 1 GBaud. Then, a variable optical attenuator (VOA) is used to adjust the modulation variance V_A, and the optical DMCS signal can be achieved. The SOP of the optical DMCS signal is controlled by a polarization controller (PC) and aligns with the principal axis of the polarization beam combiner (PBC). The reference path mainly consists of an optical delay line, VOA, and PC. In the transmission link, 25 km SSMF is used in the laboratory environment. Before being launched into the receiver, the SOP of the optical signal is continuously scrambled by General Photonic PSY-201. At Bob's site, another independent running CW laser with a linewidth of <100 Hz is used as the local oscillator, and the center wavelength is about 1.75 GHz shift from CW laser 1. Then, the optical signal and local oscillator are coherently detected by a polarization diversity receiver. The 3dB bandwidth, responsibility, and gain of the BPD are 1.6 GHz, 0.85 *A*/*W*, and 1.6×10^4 *V*/*A*, respectively. Finally, the received electrical signals are digitalized by a digital storage oscilloscope (DSO) at 10 GSa/s, and offline DSP as shown in Fig.1 is performed for raw key recovery.

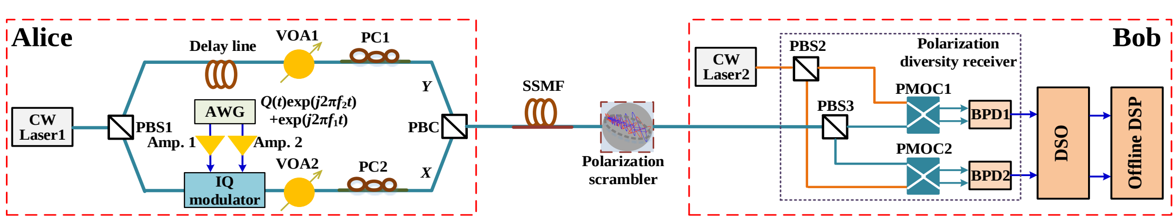

Fig. 2 The experimental setup of LLO CV-QKD to evaluate the performance of the proposed algorithm.

Figure 3 shows the experimental results of measured excess noise and calculated SKRs at different polarization scrambling rates (SRs) to evaluate the polarization tracking performance of the proposed algorithm. Here, 20 tests have been performed at each SR, and the excess noise is estimated using the linear channel model with a block size of 1×10^6. Fig. 3(a) shows the excess noise performance under different SRs, and the fluctuation of excess noise is around 0.02-0.06 in the shot noise unit (SNU). The pink stars are the mean value of excess noises, and they are 0.038, 0.038, 0.043, 0.052, and 0.048 SNU under SR of 0.63, 1.26, 3.14, 6.28 and 12.57 krad/s, respectively. Fig. 3(b) shows the excess noise performance under SR=12.57krad/s (i.e., the fastest SR of PSY-201) when the fast polarization tracking algorithm is used or not, and the results of SR=0 are given as a reference. As can be seen from Fig. 3(b), the fluctuation of excess noise for SR=0 and 12.57 krad/s are similar when fast polarization tracking is used, and the excess noise is unacceptable without fast polarization tracking. Fig. 3(c) shows the experimental results of achieved SKR under different SRs. The curve represents the asymptotic SKR bound by utilizing the parameters of SR=0 where the modulation variance, excess noise, and loss of fiber link are 6.15 SNU, 0.030 SNU, and 4.971 dB, respectively. Furthermore, the quantum efficiency of the receiver η = 0.56, the electronic noise V_{ele} = 0.15 SNU, reconciliation efficiency β = 0.95, and the ratio of training sequence is set to 20%. Dots in Fig. 3(c) represent the experimental measured averaged SKRs, which are calculated by a similar method in Ref. [8]. From Fig. 3(c), it is hard to distinguish the SKRs for different SRs. The asymptotic SKRs are 51.60, 45.98, 46.66, 43.82, 39.56, and 42.14 Mbps at SR of 0, 0.63, 1.26, 3.14, 6.28, 12.57 krad/s, respectively. In this case, the proposed fast polarization tracking algorithm is effective for correcting fast or bursting SOP perturbation.

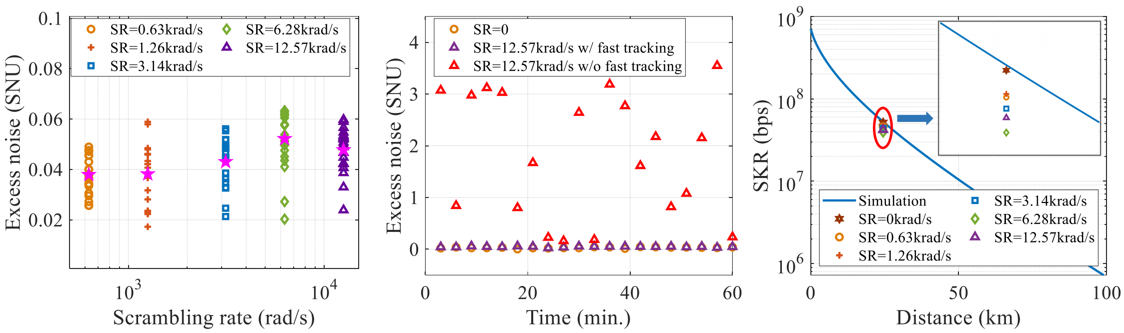

(a) (b) (c)

Fig. 3 The polarization tracking performance of the proposed algorithm for LLO CV-QKD. (a) the excess noise performance at different SRs, (b) the excess noise performance at SR=12.57krad/s with and without fast polarization tracking algorithm, and (c) the SKR performance at different SRs.

4. Conclusion

A simple and fast polarization tracking algorithm is experimentally demonstrated for LLO CV-QKD system. The results of excess noise and SKR for DG-256QAM after transmission of 25-km SSMF are given, which shows the proposed algorithm has a good performance for the LLO CV-QKD system. More importantly, the algorithm performance is tested under different SRs, which is a big challenge for demultiplexing the quantum signals. The results show that the performance of excess noise and SKR are remarkable when the SR is 12.57 krad/s. Theoretically, the algorithm will still work for higher SR. Consequently, the proposed fast polarization tracking algorithm has the potential for improving the flexibility and stability of LLO CV-QKD.

5. Acknowledgements

We acknowledge financial support from the National Key Research and Development Program of China (2020YFA030970X); The National Science Foundation of China (61901425, 62101516, 62171418, U19A2076); the Chengdu Major Science and Technology Innovation Program (2021-YF08-00040-GX); the Chengdu Key Research and Development Support Program (2021-YF05-02430-GX, 2021-YF09-00116-GX); the Technology Innovation and Development Foundation of China Cyber Security (JSCX2021JC001); the Sichuan Application and Basic Research Funds (2021YJ0313); the Sichuan Science and Technology Program (2019JDJ0060, 2020YFG0289, 2022YFG0330); National Science Key Lab Fund Project (6142103200105).

6. Reference

[1] F. Grosshans et al., Phys. Rev. Lett., 88(5), 057902, 2002.
[2] D. Waddy et al., Photonic. Tech. L., 13(9), pp.1035-1037, 2001.
[3] W. Liu et al., Phys. Rev. A, 102, 032625, 2020.
[4] T. Eriksson et al., JLT, 38(8), pp. 2214-2218, 2020.
[5] T. Wang et al., Opt. Express, 27(19), pp. 26689–26700, 2019.
[6] A. Denys et al., Quantum, 5, pp. 540-579, 2021.
[7] N. Cui et al., Opt. Express, 26(16), pp. 21170-21183, 2018.
[8] Y. Pan et al., Opt. Lett., 47(13), pp. 3307-3310, 2022.